Neuropsychologia 59 (2014) 112–123

Contents lists available at ScienceDirect

Neuropsychologia

journal homepage: www.elsevier.com/locate/neuropsychologia

Dissociating contributions of ACC and vmPFC in reward prediction, outcome, and choice

Eliana Vassena [a,b,*], Ruth M. Krebs [a], Massimo Silvetti [a,b], Wim Fias [a,b], Tom Verguts [a,b]

[a] Department of Experimental Psychology, Ghent University, Henri Dunantlaan 2, B-9000 Ghent, Belgium
[b] GIfMI, Ghent Institute for Functional and Metabolic Imaging, Ghent University Hospital, De Pintelaan 185B, B-9000 Ghent, Belgium

ARTICLE INFO

Article history:
Received 4 January 2014
Received in revised form
28 April 2014
Accepted 29 April 2014
Available online 9 May 2014

Keywords:
ACC
vmPFC
Prediction error
Outcome
Value
Choice

ABSTRACT

Acting in an uncertain environment requires estimating the probability and the value of potential outcomes. These computations are typically ascribed to various parts of the medial prefrontal cortex (mPFC), but the functional architecture of this region remains debated. The anterior cingulate cortex (ACC) encodes reward prediction and outcome (i.e. win vs lose, Silvetti, Seurinck, & Verguts, 2013. Cortex, *49*(6), 1627–35. doi:10.1016/j.cortex.2012.05.008). An outcome-related value signal has also been reported in the ventromedial Prefrontal Cortex (vmPFC, Rangel & Hare, 2010. Current Opinion in Neurobiology, 20(2), 262–70. doi:10.1016/j.conb.2010.03.001). Whether a functional dissociation can be traced in these regions with respect to reward prediction and outcome has been suggested but not rigorously tested. Hence an fMRI study was designed to systematically examine the contribution of ACC and vmPFC to reward prediction and outcome. A striking dissociation was identified, with ACC coding for positive prediction errors and vmPFC responding to outcome, irrespective of probability. Moreover, ACC has been assigned a crucial role in the selection of intentional actions (decision-making) and computing the value associated to these actions (action-based value). Conversely, vmPFC seems to implement stimulus-based value processing (Rudebeck et al., 2008. Journal of Neuroscience, *28*(51), 13775–85. doi:10.1523/JNEUROSCI.3541-08.2008; Rushworth, Behrens, Rudebeck, & Walton, 2007. Trends in Cognitive Sciences, 11(4), 168–76. doi:10.1016/j.tics.2007.01.004). Therefore, a decision-making factor (choice vs. no choice condition) was also implemented in the present paradigm to distinguish stimulus-based versus action-based value coding in the mPFC during both decision and outcome phase. We found that vmPFC was more activated during the outcome phase in the no-choice than in the choice condition, potentially confirming the role of this area in stimulus-based (more than action-based) value processing.

1. Introduction

Humans constantly face Hamlet's dilemma in everyday life. Would you prefer a reliable job with a steady income over working on commission for high bonuses? Would you invest your savings in a pension fund or buy high-leveraged derivatives at the risk of a considerable loss? Adaptively choosing between an uncertain high profit versus a certain but smaller one involves predicting the probability of the profit, selecting one of the options, and verifying the outcome.

Foreseeing and detecting benefits are adaptive skills, essential in driving goal-directed behavior. In the human and in the non-human primate brain, these computations are mediated by the medial prefrontal cortex (mPFC, Haber & Knutson, 2010). The mPFC computes the expectation of an upcoming reward (i.e. reward prediction), as well as the violation of this expectation (Amiez, Joseph, & Procyk, 2006; Jessup, Busemeyer, & Brown, 2010; Knutson & Cooper, 2005; Matsumoto, Matsumoto, Abe, & Tanaka, 2007; Silvetti, Seurinck, & Verguts, 2013). This violation is often termed prediction error and it occurs when an outcome is better (positive prediction error, PPE) or worse than expected (negative prediction error, NPE) (Sutton & Barto, 1998). However, several other related functions have been ascribed to the mPFC besides reward prediction and prediction error, such as integrating reward with potential associated costs, driving decision making (selecting among different available options) and computing the value of possible outcomes (Nee, Kastner, & Brown, 2011; Rushworth & Behrens, 2008).

A major point in this debate concerns the functional architecture of the mPFC (Bush et al., 2002; Shackman et al., 2011). On the one hand, the anterior cingulate cortex (ACC) plays a critical role in reward prediction and prediction error coding (Jessup et al., 2010; Kennerley, Behrens, & Wallis, 2011; Silvetti et al., 2013). On the other hand, a complementary role in outcome coding has been

* Corresponding author at: Department of Experimental Psychology, Ghent University, Henri Dunantlaan 2, B-9000 Ghent, Belgium. Tel.: +32 9 264 6439.
E-mail address: Eliana.Vassena@UGent.be (E. Vassena).

http://dx.doi.org/10.1016/j.neuropsychologia.2014.04.019
0028-3932/

hypothesized for ventromedial prefrontal cortex (vmPFC, Kennerley & Wallis, 2009; O'Doherty, Deichmann, Critchley, & Dolan, 2002; Rushworth, Noonan, Boorman, Walton, & Behrens, 2011), which seems to establish stimulus-outcome associations and encode rewarding features (i.e. value) of a stimulus (Bartra, Mcguire, & Kable, 2013; Chib, Rangel, Shimojo, & O'Doherty, 2009; Grabenhorst & Rolls, 2011; Sescousse, Caldú, Segura, & Dreher, 2013). This suggests a regional specialization within the mPFC with respect to reward prediction, prediction-error computation and outcome coding (Hare, Doherty, Camerer, Schultz, & Rangel, 2008). However, this hypothesis has not been directly tested in humans.

Another core aspect of decision making is action selection, and it also has been attributed to the mPFC (Brass & Haggard, 2007; Holroyd & Coles, 2008; Venkatraman & Huettel, 2012). Often this process is modulated by reward prediction, as selecting riskier options (low probability of reward) seems to be associated with increased mPFC involvement (see Platt & Huettel, 2008 for a review). However, how action selection is linked to reward prediction and outcome computation across different phases of the decision-making process still lacks a systematic account.

To tackle these issues, the present fMRI experiment manipulated reward prediction, outcome, and choice to systematically characterize the functional architecture within the mPFC. In a gambling task, participants were confronted with two options in each trial, namely a gamble and small sure win. The gamble induced a reward prediction that would be sometimes violated, causing prediction errors. In half of the cases, participants could select the preferred option (choice condition) while in the other half, one option would be selected by the computer (no-choice condition).

A whole-brain analysis was performed to identify prediction-error- and value-related signals. A subsequent set of ROI analyses aimed at disentangling regional specificity of this signal throughout the mPFC across different conditions and different phases. Further analyses also elucidated the contribution of mPFC to action selection by comparing choice and no-choice conditions during both decision and outcome phase.

2. Materials and methods

2.1. Participants

Twenty-three healthy volunteers participated in this experiment (12 females). Two subjects were excluded from further analyses due to excessive head motion (more than 3 mm motion in either rotation or translation). One subject was excluded from further analysis due to poor task performance: This participant never selected the gamble options in the choice condition, thus failing to provide data for the prediction-error conditions of interest (see Section 2.2 for a detailed description of the paradigm). The reported results are thus based on 20 participants with a mean age of 21.9 (range 20–26). The experimental protocol was approved by the Ethical Committee of the Ghent University Hospital. All participants signed an informed-consent form before the experiment, and confirmed they had no neurological or psychiatric history.

2.2. Experimental procedure

A gambling task was designed, adapting the paradigm used by Jessup et al. (2010). At the start of every trial, two options were presented on the screen, namely a gamble and a sure win (Fig. 1). Both options consisted of probability pies, where the grey slice indicated the probability of winning while the black slice showed the probability of not winning anything (defined from now on as losing for simplicity). Within the grey slice a number was presented, indicating the current amount of money at stake. One option was always the "sure win" pie, which was completely grey. The participants were informed that the size of the color pies indicated the probability of the events of winning or losing, without explicitly mentioning the exact probabilities. Thus the gamble pies were used to produce different prediction-error conditions.

Two types of gamble were presented: a risky gamble with a low probability of winning but a very high pay-off; and a safer gamble with a high probability of winning but a lower pay-off (Fig. 1). Importantly, the expected value of the gamble (amount of money at stake multiplied by the probability) was in each case approximately equal to the sure win option. In order to introduce some variability to make the task more engaging, in the risky gamble the potential win varied between 110 and 114 cents with a 5% probability of winning. In the safer gamble it varied between 12 and 16 cents with a 80% probability of winning. As a consequence, winning a risky gamble would produce a positive prediction error (unexpected win) while losing a risky gamble would represent a fulfilled prediction (expected loss). Conversely, winning a safe gamble would reflect an expected win while losing a safe gamble would evoke a negative prediction error (unexpected loss). The probability indicated by the safer gamble pie was always reliable. The probability indicated by the risky gamble pie was in fact slightly higher (shown probability 5%, actual probability 10%), in order to allow the participant to experience the positive prediction error situation in a sufficient number of trials. At the end of the experiment participants were asked if they found the probabilities shown by the pies reliable, which was the case for everyone.

On top of the prediction-error manipulation, choice was introduced in the design as additional factor. In half of the trials, participants were given the possibility to select their preferred option (choice condition), while in the remaining trials one of the options would be randomly selected by the computer (no-choice condition, with half of no-choice trials giving the automatic selection of a gamble, and half of a sure win). In order to maximize visual similarities in the two conditions, a no-choice trial was signaled by two arrows presented between the pies pointing in the same direction, indicating the option to be selected, whereas in a choice trial two arrows pointing in opposite directions were displayed on top of each other (Fig. 1). The presentation was randomized and the conditions were fully crossed (each gamble type appeared the same number of times in the choice and in the no-choice condition).

In order to keep the timing of the motor response as comparable as possible in both choice and no-choice condition, participants had to wait for a go-signal after the presentation of the pies. The response execution was followed by a randomly jittered interval (2 to 4 s, mean 3 s). Subsequently, the outcome was displayed, indicating the respective win or loss. The post-outcome inter-trial interval was also jittered (pseudo-exponential distribution ranging from 600 ms to 8 s, mean 4 s). The entire experiment consisted of 288 trials divided in three blocks, for a total duration of 60 min. The different trial types were randomly interleaved to be suitable for event-related analysis. During the break between blocks, the participants were asked via headphones to estimate how well they thought they were performing, in order to keep subjects focused on the task.

2.3. fMRI data acquisition

Structural and functional images were acquired through a 3 T Magnetom Trio MRI scanner (Siemens), using a 32-channel radio-frequency head coil. First, an anatomical T_1 weighted sequence was collected, resulting in 176 high-resolution slices (TR=1550 ms, slice thickness=0.9 mm, voxel size=$0.9 \times 0.9 \times 0.9$ mm, FoV=220 mm, flip angle=9°). Subsequently, functional images were acquired using a T_2^* weighted EPI sequence (30 slices per volume, TR=2000 ms, slice thickness=3 mm, distance factor=17%, voxel size=$3.5 \times 3.5 \times 3.0$ mm, FoV=224 mm, flip angle=80°). On average 550 volumes per run were collected during 3 runs.

2.4. fMRI data analysis

The first 4 volumes of the functional scans were discarded to allow for steady-state magnetization. The data were preprocessed with SPM8 (http://www.fil.ion.ucl.ac.uk/spm). Images were realigned to the first image of the run. The structural T_1 image was coregistered to the functional mean image to allow a more precise normalization. The unified segmentation and nonlinear warping approach of SPM8 was applied to normalize structural and functional images to the MNI template (Montreal Neurological Institute). Functional images were then smoothed with a Gaussian kernel of 8 mm full width half maximum (FWHM).

Subsequently a General Linear Model (GLM) was applied in order to identify each subject's condition-specific activation. Three factors were manipulated, namely probability of winning (low, high), outcome (lose, win), and choice (choice, no choice). This was applied to both decision phase and outcome phase. Hence, sixteen different conditions were modeled, crossing probability of winning (low/high), outcome (win/lose), choice (choice/no choice), and phase (decision/outcome). The factors probability of winning and outcome together define expected loss (low probability of winning+lose), positive prediction error (low probability of winning+win), negative prediction error (high probability of winning+lose), and expected win (high probability of winning+win).

Trials in which participants selected the sure win were modeled separately and were not considered for further analysis (as in Jessup et al., 2010). One regressor of no interest was added to model trials in which errors were made, namely when in the no-choice condition the response did not match the instructed response, thus excluding error-related activation from the analysis. Six subject-specific regressors were added modeling motion parameters obtained from the realignment. The resulting stimulus functions were convolved with the canonical hemodynamic response function. To account for low frequency noise a 128 s high pass filter was included. To account for serial auto-correlation, an autoregressive model was applied.

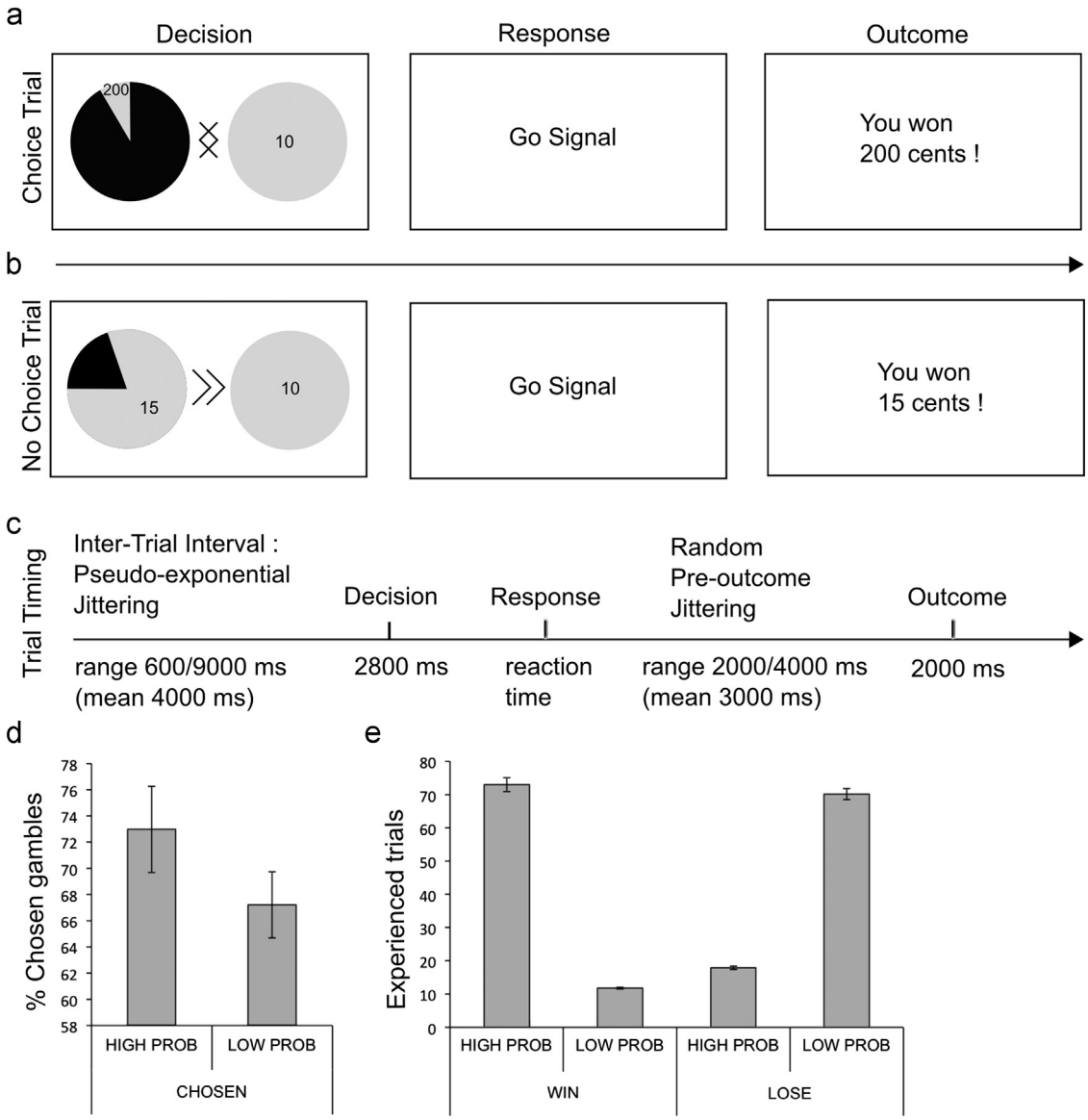

Fig. 1. Task structure and behavioral results. During the decision phase, two options are presented on the screen. Each option represents the probability of winning (in grey; but in orange in the actual experiment) a certain amount of money (in cents, written in the grey slice). The complementary (in black; but in blue in the actual experiment) part of the pie is the probability of not winning on that trial. After 2800 ms, a go signal is presented, and the participant can choose one of the two pies. Subsequently the outcome is presented (win or lose). (a) Example of a trial in the choice condition: when the central arrows are pointing in the opposite direction, the participant can freely decide which option to pick. In this example, the gamble option is risky (low probability of winning) with a high pay-off. Note though that the factor gamble type (low/high winning probability) was systematically crossed with factor choice/no choice. (b) Example of a trial in the no choice condition: the participant is forced to select the option indicated by the two arrows. In this example, the gamble option is safe (high probability of winning) with a low pay-off. (c) Trial timing: the Inter-trial Interval is jittered in a pseudo-exponential fashion, ranging from 600 to 9000 ms (mean 4000). The duration of the decision phase is 2800 ms. As the go signal appears, the participant is allowed to respond. A randomly jittered interval precedes the outcome (range 2000/4000 ms, mean 3000 ms). The outcome presentation concludes the trial and its duration is 2000 ms. (d) Percentage of chosen gambles (over the sure win), for the high probability of winning gamble (HIGH PROB) and the low probability of winning gamble (LOW PROB). (e) Average number of experienced trials per condition. In both plots, error bars denote 1 standard error of the mean. (For interpretation of the references to color in this figure legend, the reader is referred to the web version of this article.)

At the second level, we first concentrated on the *outcome phase*. A random-effects analysis was performed. A $2 \times 2 \times 2$ factorial design was modeled, with choice (choice/no choice), outcome (lose/win) and probability of winning (low/high) as factors. All the reported whole-brain results where subjected to a voxel-level threshold of 0.001 uncorrected and survived a cluster-level family-wise error (FWE) correction for multiple comparisons with a *p*-value of 0.05. First, the main contrasts were computed, namely main effect of choice, main effect of outcome, main effect of probability, and outcome by probability interaction (prediction-error-related activity, cf. Jessup et al., 2010). It should be noted that the focus was on the interaction contrast, in order to identify prediction-error signals. The contrast reflecting the main effect of probability is in fact not optimized in this design, as it might be confounded with reward magnitude. Furthermore, additional pairwise contrasts decomposing the interaction were computed.

Subsequently the main goal of the study was addressed, namely a precise identification of the respective contributions of ACC and vmPFC to the response to reward prediction, outcome and choice. These areas have often been reported to be implicated in one or more of these processes. Therefore, as strongly hypothesis-driven approach, two region-of-interest (ROI) analyses were performed. First a functional ROI approach was adopted, where two ROIs were defined on the basis of previous studies. Importantly this guarantees an unbiased selection with respect to the whole-brain significant prediction error and outcome signals. The ROI encompassing the vmPFC was defined on the basis of a meta-analysis performed on several imaging studies involving reward (Liu, Hairston, Schrier, & Fan, 2011). In that study, two clusters are reported in the medial Orbito-Frontal Cortex (mOFC, left and right) to be activated when receiving a positive outcome. As a note, the anatomical definition of mOFC and vmPFC in fMRI studies overlap (Rushworth

et al., 2011). We centered the vmPFC ROI ($20 \times 10 \times 10$ mm) on the averaged coordinates from left and right mOFC from Liu et al. (2011), in order to encompass both left and right vmPFC (MNI coordinates $x=0$ $y=51$ $z=-10$), as no specific lateralization could be hypothesized from previous evidence. The ROI targeting the ACC was derived from the study of Nee et al. (2011), where a systematic analysis of mPFC was carried out. The ACC ROI was not defined on the basis of Liu et al. because the factor probability was not included in that meta-analysis. Conversely, after identifying whole-brain effects, Nee et al. defined multiple ROIs from previous studies investigating different functions attributed to the ACC, among which conflict processing and error monitoring. One area was defined as anterior rostro-cingulate zone (aRCZ). This proved to be the area most sensitive to unexpected events. For this reason this seemed to be the most appropriate ROI selection, as we were targeting prediction-error coding. It should be noted that a recent meta-analysis focused on prediction error (Garrison, Erdeniz, & Done, 2013), but only studies involving model-based fMRI were included, thus making it not the most appropriate comparison for the current paradigm. Further research should focus on studies testing prediction error in decision-making paradigms (i.e. Jessup et al., 2010) and perhaps perform ad-hoc meta-analysis (Wager, Lindquist, & Kaplan, 2007), thus granting an even more functionally precise ROI selection. To our knowledge, only a small number of studies addressed prediction-error under these conditions, thus making a meta-analysis currently unreliable. For these reasons the ROI from Nee et al. was selected. We centered our ACC ROI (also $20 \times 10 \times 10$ mm) on the coordinates of the aRCZ-ROI (MNI coordinates $x=0$ $y=28$ $z=31$). As for the vmPFC, no laterality hypothesis could be formulated and therefore the ROI covers symmetrically left and right ACC (as displayed in Fig. 3a).

Second, an anatomical ROI approach was adopted, in order to provide convergent evidence for the previous analysis, to grant a more systematic and extensive sampling of the whole mPFC surface, and to ensure unbiased selection. Six box-shaped ROIs (10 mm wide) were anatomically defined sampling across the entire mPFC, starting from the posterior boundary of the Anterior Cingulate Cortex (ACC), as defined by the Brodmann area 24. The ROIs were medially centered, in order to sample from both left and right mPFC. The subsequent selection of regions was determined by progressively shifting the ROI center along the rostro-caudal axis. In order to follow the anatomical architecture of the mPFC the center of the two more rostral ROIs was also shifted lower on the dorso-ventral axis to cover peri-genual ACC and ventromedial prefrontal cortex (vmPFC, see Fig. 4a). As a result, 6 ROIs were obtained, 4 lying within the caudal to medial part of the ACC, one covering the peri-genual cingulate cortex, and one encompassing the vmPFC.

Condition-specific activation (percent signal change) was extracted from each ROI (both functional and anatomical) using the Marsbar Toolbox (Brett, Anton, Valabregue, & Poline, 2002) and submitted to a repeated-measures analyses of variance.

Subsequently, a separate second-level analysis was performed focusing on the *decision phase*, i.e. time-locked to the onsets of the display showing the pies. Specifically, a random-effects analysis was performed by implementing a 2×2 factorial design, with choice (choice/no choice) and probability of winning (low/high) as factors. The probability of winning could be 5% (low), leading to a risky gamble; or 80% (high), leading to a safe gamble. The voxel level threshold was set to 0.001 uncorrected and FWE cluster-level correction for multiple comparisons was applied, with a p-value of 0.05. Moreover, the same functional ROI procedure used for the outcome phase, was applied to the decision phase, to better characterize contributions of these areas to decision-making as well.

3. Results

3.1. Behavioral results

Subjects chose the uncertain option over the sure win on 60% of the trials. On average, participants chose 47.05 ($\pm$15.82) of the risky gambles (67.14% of the total) and 54 ($\pm$21.78) of the safe gambles (72.97% of the total, Fig. 1d). The frequency of selection of the safe gamble over the sure win did not differ significantly from the frequency of selection of the risky gamble over the sure win ($t_{(19)}=.737$, $p=.47$). As a result, participants experienced on average 11.8 ($\pm$2.69) low probability+win trials, 17.9 ($\pm$4.41) high probability+lose trials, 73 ($\pm$18.35) high probability+win trials, and 70.15 ($\pm$14.73) low probability+lose trials (Fig. 1e).

3.2. Outcome-phase whole-brain fMRI results

The activation results during the outcome phase are reported in Table 1.

The outcome contrast (win > lose) activated the vmPFC, ACC, striatum bilaterally, DLPFC bilaterally, brainstem, Posterior Cingulate Cortex (PCC) (Fig. 2a). In the reverse outcome contrast (lose > win), no clusters survived. The probability contrast (low probability > high probability) activated the ACC, pre-SMA, brainstem, striatum bilaterally and insula bilaterally. The activation in this contrast is, however, difficult to interpret as probability covaries with reward magnitude in the present design. The contrasts computed for the main effect of probability and the main effect of outcome elicited a widespread whole-brain level activation. This resulted in big clusters, potentially invalidating the regional validity of the cluster-level inference (Woo, Krishnan, & Wager, 2014). For this reason, the voxel-wise FWE ($p=.05$) corrected results are also reported (see Table 1).

The whole-brain prediction error contrast (whole-brain interaction outcome by probability) yielded a consistent activation in the ACC, bilateral insula, bilateral striatum, brainstem and pre-SMA (Fig. 2b). This pattern consistently reflects activity elicited by unexpected outcomes in previous studies (Jessup et al., 2010; Nee et al., 2011; Silvetti et al., 2013).

In a next step, in order to explore differences and commonalities in outcome and reward prediction coding, the prediction error contrast (outcome by probability interaction) and the outcome contrast (win > lose) were plotted together in Fig. 2c. This showed partial overlap (displayed in violet) of outcome (in red) and prediction error (in blue). From this plot one can detect a first indication of selectivity for outcome versus prediction error coding along the mPFC; however, this claim remains exploratory at the whole-brain level. In the following section, the targeted ROI analyses will be discussed, providing a systematic and statistically sound investigation of different contributions of vmPFC and ACC.

Furthermore, the pairwise contrasts decomposing the interaction were computed (low probability+win > high probability+win, high probability+lose > low probability +lose). These contrasts revealed that the interaction pattern was mainly driven by the response to low probability+win outcomes (Fig. 2e), as further clarified by the ROI analysis (see below). This seems to highlight a power problem to detect prediction error related activity in the high probability+lose outcomes. Jessup et al. (2010), from which our paradigm was adapted, found such a pattern for the analogous contrast in the Insula and the ACC. The reasons for these discrepancies should be investigated in further research.

Finally, a main effect of choice condition was reported. In particular a stronger response in the no-choice condition was observed in the vmPFC (Fig. 2d) and in the left temporo-parietal junction (TPJ). Note that the main effect in the vmPFC was driven by a difference in deactivation (Fig. 3e), as it is commonly found in this region (Raichle et al., 2001). As further noted by Rushworth et al. (2011, p. 1057), "activations reported in vmPFC actually correspond to different degrees of deactivation".

3.3. Outcome-phase functional ROI analysis

The planned ROI analysis was performed on the outcome-phase prediction-error signal. The goal of this approach was to better characterize the whole-brain results, targeting ACC and vmPFC function in reward prediction, outcome and choice coding. This analysis was guided by the a-priori hypothesis formulated on the basis of previous evidence, that ACC would encode reward prediction and prediction error, while the vmPFC would encode the outcome (Jessup et al., 2010; Rushworth et al., 2011). With this approach, we were able to contrast directly vmPFC and ACC activity by testing the specific hypothesis of a functional segregation within the mPFC for prediction error vs. outcome coding. The percent signal change scores showed a clear contribution of the ACC to the prediction-error signal (Fig. 3), where the strongest response was elicited by the positive unexpected outcome (Fig. 3d). This was confirmed by a significant outcome by probability interaction ($F_{(1,19)}=15.07$. $p=.001$), irrespective of choice (no three-way

Table 1
Summary of the activations in the whole brain contrasts. Contrasts in the outcome phase: No Choice > Choice, Prediction Error (interaction outcome by probability). Contrasts in the decision phase: Choice > No Choice, No Choice > Choice, Risky Gambles > Safe Gambles (low probability of winning > high probability of winning), Risk-preference as a covariate for Prediction Error. Cluster-level contrast values are presented with family-wise error correction applied (p-FWEcor), and false-discovery rate correction are applied (p-FDRcor).

Area	MNI coordinates *x y z*	Cluster-level *few*	Cluster-level *FDR*	Cluster *size*	Peak *T*
Outcome Phase					
Outcome (*win* > *lose*)					
Left pallidum	−12 6 −2	0.000	0.000	43399	9.42
Right pallidum	12 10 −2				8.79
Putamen	18 4 −8				8.43
Inferior temporal gyrus	−52 −54 10	0.001	0.001	541	7.43
Occipital cortex	−18 −96 −2	0.002	0.001	507	5.62
Outcome (*win* > *lose*) *voxel-wise FWE*					
Left pallidum	−12 6 −2	0.000	0.000	5052	9.42
Right pallidum	12 10 −2				8.79
Putamen	18 4 −8				8.43
Left inferior frontal operculum	−44 6 26	0.000	0.000	1712	7.98
Inferior frontal gyrus	−38 34 10				6.82
	−46 44 14				6.64
Anterior cingulate cortex	−6 34 6	0.000	0.000	3355	7.76
	8 28 14				7.67
	0 38 −2				7.53
Right inferior frontal operculum	44 10 26	0.000	0.000	1123	7.55
Right inferior frontal gyrus	44 36 16				6.18
Inferior temporal gyrus	−52−54−10	0.000	0.000	186	7.43
Occipital cortex	28 −92 −4	0.000	0.000	527	7.41
Inferior occipital gyrus	40 −82 −10				6.88
Right inferior temporal gyrus	56 −52 −12	0.000	0.000	289	7.22
Poster cingulate gyrus	8 −36 32	0.000	0.000	472	7.14
Angular gyrus	32 −58 42	0.000	0.000	1185	6.84
Right precuneus	36 −70 34				6.57
Right inferior parietal lobule	46 −36 48				5.97
Left inferior parietal lobule	−50 −38 44	0.000	0.000	1347	6.55
Supramarginal gyrus	−42 −44 38				6.06
Precuneus	8 −56 18	0.000	0.000	277	5.29
	−8 −50 14				5.09
Mid-cingulate gyrus	−6 −6 32	0.000	0.000	242	6.23
	6 0 30				6.02
	6 10 2				5.62
Superior frontal gyrus	−26 22 56	0.000	0.000	398	6.2
Middle frontal gyrus	−26 12 62				5.94
	−28 34 48				5.54
Hippocampus	32 −10 −10	0.004	0.095	25	5.69
Occipital cortex	−18 −96 −2	0.000	0.002	100	5.62
Probability (*low probability* > *high probability*)					
Right insula	30 24 −6	0.000	0.000	23705	9.35
Left insula	−28 18 −4				8.83
Anterior cingulate cortex	8 36 14				8.03
Inferior parietal lobule	−30 −50 44	0.000	0.000	4684	5.63
Precuneus	30 −60 30				5.46
Supramarginal gyrus	46 −44 30				5.23
Inferior temporal cortex	−44 −58 −10	0.001	0.001	534	5.2
Fusiform gyrus	−36 −64 −8				4.78
Left occipital cortex	−18 −98 −6	0.025	0.015	274	3.99
Right occipital cortex	30 −88 2	0.035	0.016	250	3.93
Probability (*low probability* > *high probability*) *voxel-wise FWE*					
Right insula	30 24 −6	0.000	0.000	4756	9.35
Left insula	−28 18 −4				8.83
Thalamus	8 −8 2				7.37
Anterior cingulate cortex	8 36 14	0.000	0.000	2270	8.03
	−6 34 14				7.09
	6 32 24				6.69
Middle frontal gyrus	48 10 50	0.000	0.000	262	6.8
Righ precentral gyrus	48 10 34				5.53
Posterior cingulate cortex	−4 −28 28	0.000	0.000	384	6.62
Middle frontal gyrus	28 56 0	0.000	0.022	60	5.68
Inferior parietal lobule	−30 −50 44	0.000	0.001	150	5.63
Superior frontal gyrus	22 48 34	0.003	0.101	31	5.46
Precuneus	32 −70 30	0.000	0.000	164	5.46
Angular gyrus	30 −56 44				5.08
Left precentral gyrus	−46 2 54	0.013	0.340	10	5.25
Supramarginal gyrus	46 −44 30	0.004	0.126	26	5.23
Inferior temporal cortex	−44 −58 −10	0.004	0.132	24	5.2

Table 1 (*continued*)

Area	MNI coordinates *x y z*	Cluster-level *few*	Cluster-level *FDR*	Cluster *size*	Peak *T*
Inferior frontal operculum	34 20 30	0.000	0.022	60	5.12
Inferior frontal gyrus	46 26 28				5.07
Prediction-error (*outcome by probability interaction*)					
Left insula	−32 22 −2	0.000	0.000	2653	8.04
	−32 14 −12				6.43
Inferior frontal operculum	−40 10 30				4.81
Right insula	32 24 −4	0.000	0.000	3845	7.79
Inferior frontal gyrus	46 20 6				5.86
Middle frontal gyrus	50 12 48				5.15
Anterior cingulate cortex	6 38 36	0.000	0.000	4453	5.87
	6 30 18				5.85
	6 30 38				5.69
Thalamus	10 −10 2	0.000	0.000	1803	5.46
Pallidum	−10 4 2				5.26
Midbrain	0 −20 −14				5.25
Posterior cingulate cortex	−6 −26 30	0.001	0.000	564	5.27
	6 −26 30				4.84
Left inferior parietal lobule	−32 −58 46	0.000	0.000	712	5.09
Angular gyrus	36 −56 42	0.000	0.000	846	4.95
	50 −60 46				4.32
Right inferior parietal lobule	54 −48 52				3.6
Righ precuneus	12 −68 36	0.005	0.002	401	4.9
Left precuneus	−8 −68 34				3.58
Middle temporal gyrus	56 −26 −10	0.016	0.005	310	4.38
	66 −40 −4				4.33
Angular gurys	56 −50 26	0.019	0.006	298	4.34
Left inferior parietal lobule	−48 −38 44	0.121	0.035	164	4.11
Positive prediction error (*low probability+win > high probability +win*)					
Left insula	−30 20 −4	0.000	0.000	35265	9.12
Right insula	32 22 −4				8.99
Midbrain	6 −24 −14				8.52
Right inferior temporal gyrus	56 −52 −12	0.001	0.000	567	6.60
Middle temporal gyrus	64 −44 −2				4.63
	58 −40 −10				4.47
Left inferior temporal gyrus	−52 −54 −10	0.003	0.001	429	6.21
Occipital cortex	26 −94 −4	0.001	0.000	570	5.61
Positive prediction error (*low probability+win > high probabilit+win*) *voxel-wise FWE*					
Left insula	−30 20 −4	0.000	0.000	2094	9.12
Right inferior frontal operculum	−40 10 28				8.23
Right insula	32 22 −4	0.000	0.000	5214	8.99
Midbrain	6 −24 −14				8.52
Left inferior frontal operculum	44 12 26				8.13
Anterior cingulate cortex	8 36 14	0.000	0.000	3363	7.90
	10 26 40				7.82
	−4 38 6				7.81
Left inferior parietal lobule	−30 −56 42	0.000	0.000	1263	7.49
Angular gyrus	36 −58 42	0.000	0.000	777	7.41
Right inferior parietal lobule	48 −40 48				5.61
Posterior cingulate cortex	6 −34 32	0.000	0.000	723	7.22
No choice > choice					
vmPFC	−6 52 −14	0.044	0.030	234	4.18
Left superior temporal gyrus	−48 −2 −14	0.019	0.030	295	4.82
Right middle temporal gyrus	64 −10 −8	0.001	0.002	576	4.38
Right precentral gyrus	48 −18 60	0.036	0.030	249	4.16
Left TPJ	−42 −74 32	0.027	0.030	271	3.94
Decision phase					
Choice > no choice					
Left and right ACC	8 26 32	0.000	0.000	6291	6.86
Right superior parietal	28 −62 38	0.000	0.000	2508	6.85
Right insula	30 26 4	0.000	0.000	582	5.60
Left superior parietal lobule	−24 −66 44	0.000	0.000	801	5.46
Left frontal superior gyrus	−24 −2 46	0.003	0.002	338	5.25
Left Insula	−24 20 6	0.000	0.000	685	5.20
Right middle frontal gyrus	44 36 20	0.012	0.006	259	4.49
Right inferior frontal gyrus	48 8 26	0.045	0.019	185	4.33
No choice > choice					
Left TPJ	−44 −60 16	0.000	0.000	1894	5.94
Right TPJ	62 −54 26	0.000	0.000	919	5.20
Left/right precuneus	−4 −56 32	0.000	0.000	478	4.22

Table 1 (*continued*)

Area	MNI coordinates *x y z*	Cluster-level *few*	Cluster-level *FDR*	Cluster *size*	Peak *T*
Risky gambles > safe gambles					
Bilateral ACC	−10 36 20	0.018	0.021	235	4.17
Right middle occipital gyrus	30 −92 −2	0.001	0.002	424	6.07
Left middle occipital gyrus	−28 −92 −8	0.074	0.043	158	5.03
Left insula	−28 −20 −4	0.079	0.043	155	4.32
Right fusiform gyrus	40 −60 −12	0.090	0.043	148	3.88

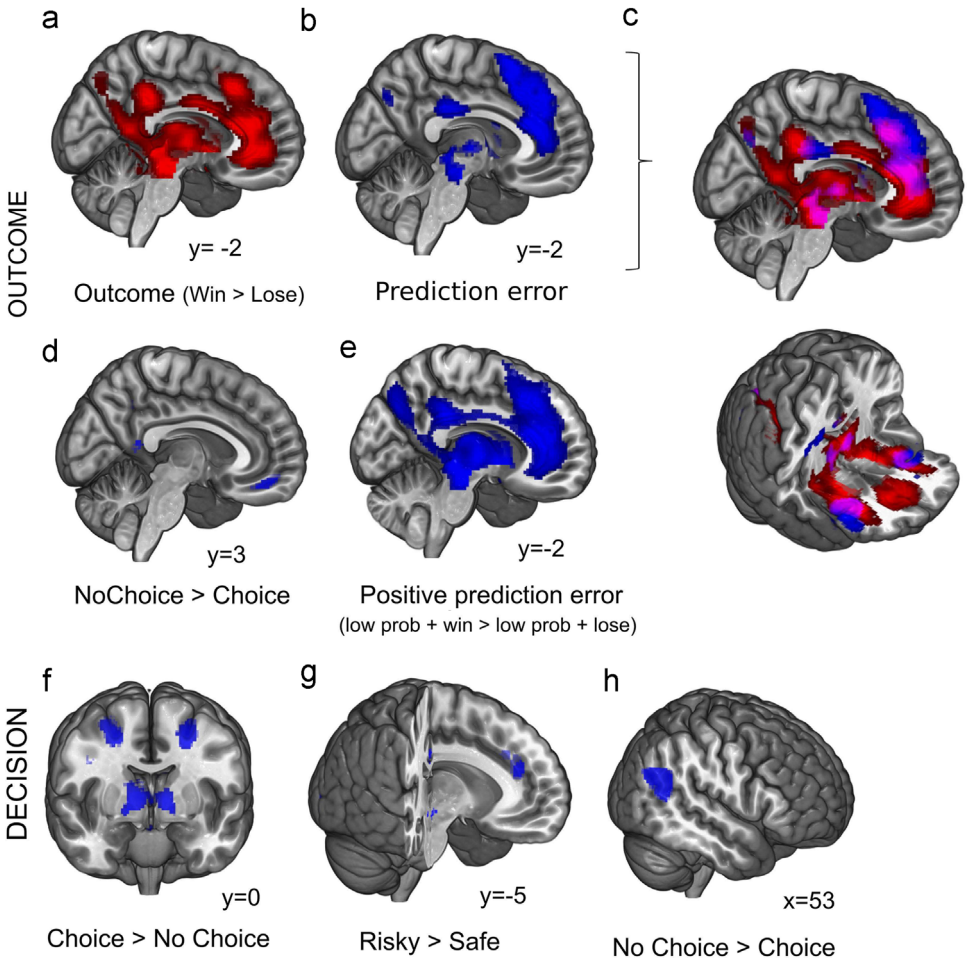

Fig. 2. Whole brain contrasts. Outcome phase: (a) Outcome contrast (Win > Lose). (b) Prediction error contrast (outcome by probability interaction). (c) Outcome contrast (in red) and prediction error contrast showing partial overlap, as well as selectivity for outcome in the vmPFC and prediction error in ACC. (d) No Choice > Choice contrast. (e) Positive prediction error contrast (low probability + win > low probability + lose). Decision Phase: (f) Choice > No Choice contrast. (g) Risky gambles > safe gambles contras. (h) No Choice > Choice contrast. (For interpretation of the references to color in this figure legend, the reader is referred to the web version of this article.)

interaction choice by outcome by probability, $F_{(1,19)}=.79$. $p=.39$). A main effect of outcome ($F_{(1,19)}=37.96$. $p<.001$) and a main effect of probability ($F_{(1,19)}=67.76$. $p<.001$) were also identified in the ACC, but these did not interact with choice either (interaction choice by outcome $F_{(1,19)}=.08$. $p=.79$, interaction choice by probability $F_{(1,19)}=3.13$. $p=.10$). The ACC thus showed the expected prediction error response (Fig. 3d), but this was mainly driven by a positive prediction error signal (low probability + win > high probability win in the choice condition $t_{(19)}=4.4$, $p<.001$, and in the no-choice condition $t_{(19)}=5.03$, $p<.001$; high probability + lose > low probability + lose $t_{(19)}=-1.59$, $p=.13$ in the choice condition and $t_{(19)}=1.29$, $p=.21$ in the no choice condition; cf. Jessup et al., 2010).

As hypothesized, the vmPFC selectively responded to positive outcome, irrespective of winning probability, thus showing no sensitivity to prediction errors (Fig. 3e). Indeed, there was a main effect of outcome in this region ($F_{(1,19)}=16.79$, $p=.001$) and no significant outcome by probability interaction ($F_{(1,19)}=.001$, $p=.98$). Interestingly the vmPFC also showed a main effect of choice ($F_{(1,19)}=13.7$. $p=.002$).

The differential sensitivity of vmPFC and ACC was confirmed by a significant three-way interaction (region by outcome by probability) when vmPFC and ACC were both included in the analysis as additional "region" factor ($F_{(1,19)}=27.634$ $p<.001$). Consistently, this analysis also reported a main effect of region ($F_{(1,19)}=43.02$.

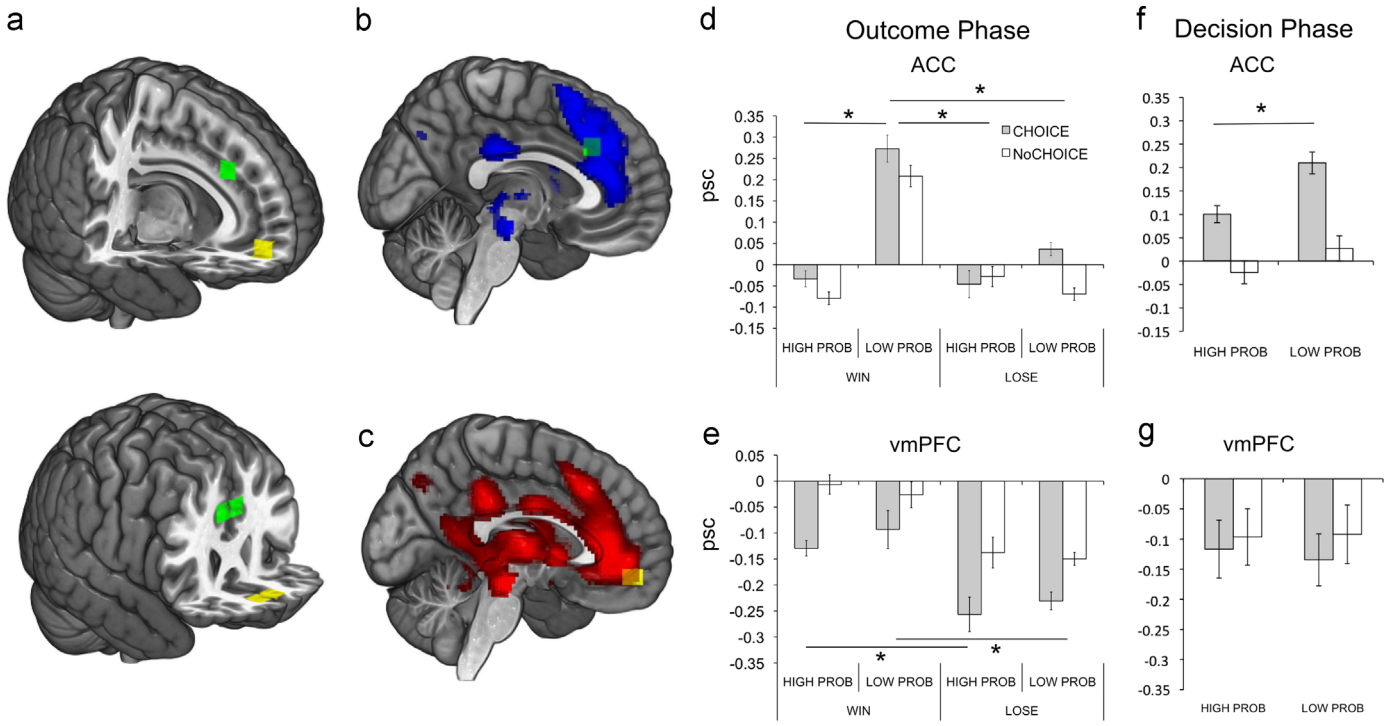

Fig. 3. Functional ROI results. (a) Region of Interest selection across the mPFC, guided by previous evidence (ACC in green, from Nee et al., 2011, vmPFC in yellow, from Liu et al., 2011). (b) ACC ROI plotted on the whole-brain prediction error contrast (outcome by probability). (c) vmPFC ROI plotted on the whole-brain outcome contrast (win > lose). (d) Percent signal change analysis in the ACC during the outcome phase: choice-condition is reported in grey, no-choice condition in white. On the *x*-axis, the other two conditions are displayed, namely outcome (WIN/LOSE) and probability of winning (HIGH PROB/LOW PROB). On the *y*-axis, the percent signal change (psc) is represented. (e) Percent signal change analysis in the vmPFC during the outcome phase: the choice condition is displayed in grey, the no-choice condition in white. On the *x*-axis, the other two conditions are displayed, namely outcome (WIN/LOSE) and probability of winning (HIGH PROB/LOW PROB). On the *y*-axis, the percent signal change (psc) is represented. (f) Percent signal change analysis in the ACC during the decision phase. (g) Percent signal change analysis in the vmPFC during the decision phase. In the plots error bars denote 1 standard error of the mean. (For interpretation of the references to color in this figure legend, the reader is referred to the web version of this article.)

$p < .001$), an interaction region by choice ($F_{(1,19)}=36.43$. $p < .001$) and an interaction region by probability ($F_{(1,19)}=17.23$. $p=.001$).

3.4. Outcome-phase anatomically-guided ROI analysis

The anatomically-guided ROI analysis was performed on the outcome phase prediction-error signal. The percent signal change scores showed a contribution of the ACC to the prediction-error signal (Fig. 4), where the strongest response was elicited by the positive unexpected outcome. Along the rostro-caudal axis, the rostro-medial portion of the ACC seemed to be the most sensitive to prediction errors, especially to the positive unexpected outcome (Fig. 4b). A significant interaction between outcome and probability was detected in the medial ACC (ROI 2, $F_{(1,19)}=6.66$, $p=.018$), in the rostro-medial ACC ($F_{(1,19)}=12.964$, $p=.002$) and in the rostral ACC ($F_{(1,19)}=13.910$, $p=.001$), irrespective of choice. These regions showed the strongest prediction error response, as one can see in Fig. 4c, where the prediction error size (as computed on the percent signal scores) is plotted as a function of anatomical location from caudal to rostral. This differential sensitivity within the ACC was confirmed by a significant three-way interaction between region, outcome and probability across the different ROIs within the ACC ($F_{(4,16)}=7.597$, $p=.001$). None of the regions showed a three-way interaction.

Strikingly, the vmPFC showed no sensitivity to prediction errors, but selectively responded to positive outcome instead, irrespective of winning probability (Fig. 3b). Indeed, there was a main effect of outcome in this region ($F_{(1,19)}=15.049$, $p=.001$) and no significant outcome by probability interaction ($F_{(1,19)}=.131$, $p=.721$).

3.5. Decision-phase whole-brain results

The results of the decision-phase analysis are summarized in Table 1. A main effect of choice was detected in the striatum (Fig. 2f) and ACC, with a stronger response in the choice condition, confirming the role of these regions in action selection (Brass & Haggard, 2007; Holroyd & Coles, 2008). Increased activation in the left and right TPJ was observed in the no choice condition (Fig. 2h).

A main effect of gamble type was also identified in the ACC (Fig. 2g), in that it was more strongly activated when participants chose the risky (i.e. low winning probability) gamble as compared to the safe gamble (high winning probability), suggesting a contribution to risk estimation as well as risk-taking behavior.

3.6. Decision-phase functional ROI analysis

An additional ROI analysis of the decision phase was performed, based on the two functionally defined ROIs used in the outcome phase. It should be noted that in this analysis the trials where the sure thing was selected were not included (as in the outcome ROI analysis). ACC showed increased activity (in terms of percent signal change) for the low probability condition as compared to the high probability condition (main effect of probability, $F_{(1,19)}=15.38$, $p=.001$). Moreover, ACC showed a main effect of choice versus no choice ($F_{(1,19)}=42.54$, $p < .001$) but no interaction ($F_{(1,19)}=1.15$, $p=.297$). This corroborates the whole brain effect during the same phase. This activation might reflect ACC contribution in undertaking risky behaviors, as it is associated in this case with choosing (voluntarily or imposed by the computer) the risky option (over the sure win). In this case it is not possible to draw

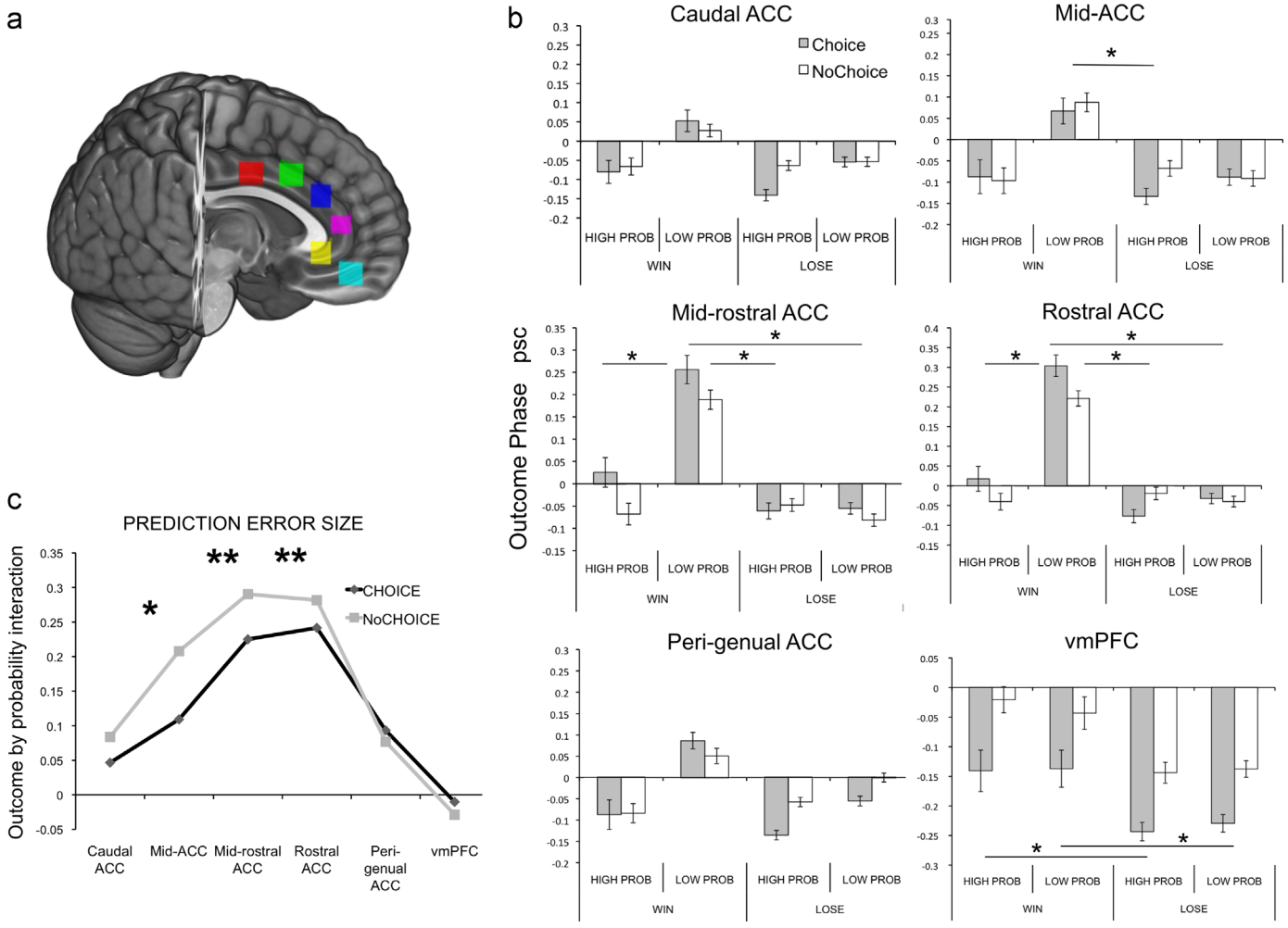

Fig. 4. Anatomical ROI analysis. (a) Anatomically-guided Region of Interest selection across the mPFC during outcome. (b). Percent signal change analysis in the six ROIs (from caudal to rostral) during the outcome phase: choice condition is reported in black, no-choice condition in grey. On the *x*-axis, the other two conditions are displayed, namely outcome (WIN/LOSE) and probability of winning (HIGH PROB/LOW PROB). On the *y*-axes the signal change (psc) is represented. In the plots error bars denote 1 standard error of the mean. (c) Prediction error size: intensity of the prediction-error-related activation in the six ROIs, from caudal to rostral, during the outcome phase. The intensity corresponds to the interaction size computed on the percent signal change scores ((low probability+win−low probability+lose)−(high probability+lose−high probability+win)). In black the choice condition is reported and in grey the no choice condition is reported. The intensity is maximal in the mid-ACC, mid-rostral ACC and rostral ACC.

conclusions regarding reward prediction, as in this design the expected value was kept constant, and this should be addressed in future research. No significant effect of choice or probability was reported in the vmPFC ROI.

4. Discussion

The current study investigated the functional architecture of the mPFC by targeting its contribution to reward prediction, outcome coding, and decision-making during a gambling task. A striking dissociation emerged between the ACC, being involved in reward prediction and (positive) prediction-error response, and the vmPFC, selectively coding for positive outcomes irrespective of probability. These findings support the hypothesis of a functional dissociation between ACC and vmPFC in prediction error and outcome coding. This idea received convergent indications from previous research but was to date not directly verified. We now discuss these and other results in the light of the current literature.

The pivotal role of mPFC in implementing and monitoring higher-order cognitive processes has been widely documented. A striking variety of different functions has been attributed to this area, ranging from reward prediction (Amiez et al., 2006; Silvetti et al., 2013), outcome coding (Rangel & Hare, 2010), reinforcement learning (Alexander & Brown, 2011; Silvetti, Seurinck, & Verguts, 2011), conflict monitoring and cognitive control (Blais & Bunge, 2010; Botvinick, Cohen, & Carter, 2004; Egner, Etkin, Gale, & Hirsch, 2008; Nee et al., 2011), to emotional regulation (Etkin, Egner, & Kalisch, 2011), prompting effortful behavior (Holroyd & Yeung, 2012; Vassena et al., 2014), and processing aversive and painful stimuli (Rainville, 1997).

Despite a wealth of research, no unifying comprehensive account has been formulated yet. The present study encompasses some elements that are traceable in most, if not all, of these different domains. Specifically, prediction errors, outcome coding, and choice are cardinal components of all goal-directed behavior, yet they have not been manipulated in the same experiment in a systematic fashion. Our design allowed investigating the role of subparts of mPFC in each of these processes, thereby contributing to a comprehensive understanding of mPFC function.

Prediction-error signals were observed in the ACC, confirming previous reports (Jessup et al., 2010; Silvetti et al., 2013), as well as in the midbrain, striatum, pre-motor supplementary area (pre-SMA), supplementary motor area (SMA) and insula (see Fig. 2b). The percent signal change analysis in the ACC revealed a sharp selectivity towards positive prediction errors, which elicited the

strongest response (see Fig. 3d). In contrast to one previous finding, negative prediction errors did not induce significant activity increases (cf. Jessup et al., 2010). As a matter of fact, single cell recordings in monkeys highlighted a difference in the distribution of prediction-error responses in the ACC, with a significantly smaller number of neurons producing a negative prediction-error signal (Kennerley et al., 2011). Furthermore, slight differences in the experimental paradigm could account for different activation patterns in our study compared to the Jessup et al. report, as the reward amounts in the current experiment were overall higher (while still respecting the proportions between conditions, and keeping the expected value constant across different options; cf. Jessup et al., 2010). The absence of negative prediction error signal might also be due to a power problem. The reward magnitude associated with the positive prediction error condition was indeed higher then in the negative prediction error condition (as in the original design of Jessup et al., 2010). A possible influence of reward magnitude cannot be completely excluded, even though the pattern emerging across different analyses (whole brain, functional ROIs, anatomical ROIs) seems to suggest a magnitude effect in the vmPFC rather than in the ACC. This issue should be addressed in further research.

ACC was involved in encoding reward prediction (see Fig. 3d and Fig. 4b). This region consistently overlaps with clusters most commonly reported in previous studies (cf. Jessup et al., 2010; Nee et al., 2011; Silvetti et al., 2013). Importantly, prediction error signals in the ACC during the outcome phase were independent of the origin of the event (i.e. the choice condition). Specifically, the selectivity for positive prediction errors persisted irrespective of whether the option was selected by the person or by the computer. This is consistent with the findings of Kool, Getz, and Botvinick (2013). In an investigation of the behavioral "illusion of control" phenomenon, these authors did not find any modulation of intentionally accepting an option on neural prediction-error activity.

In contrast, the vmPFC was insensitive to prediction errors. Instead, the vmPFC displayed an outcome coding pattern, responding more strongly to the positive outcomes, irrespective of the winning probability that was tied to the selected option (see Fig. 3e and Fig. 4b). The role of vmPFC in reward prediction, especially with respect to the outcome phase, had not been clarified yet. The vmPFC is indeed assigned a crucial function in computing outcome expectancies (Tom, Fox, Trepel, & Poldrack, 2007), which might rely on a reward prediction (or prediction error) computation. However, similar responses have been observed for obtained as well as omitted rewards in this region (Kennerley & Walton, 2011). Although it has been argued that no prediction-error signal is computed by this area, to date opposing results have also been reported (O'Doherty et al., 2002; Schoenbaum, Roesch, Stalnaker, & Takahashi, 2009; Sul, Kim, Huh, Lee, & Jung, 2010).

However, vmPFC contributions in outcome coding have been widely documented (Noonan, Kolling, Walton, & Rushworth, 2012; Rushworth, Kolling, Sallet, & Mars, 2012). Specifically, activity in the vmPFC has been shown to correlate with the subjective value attached to the stimulus by the agent (Hare, Camerer, & Rangel, 2009; Padoa-Schioppa & Assad, 2008; Plassmann, O'Doherty, & Rangel, 2007) and to reflect the value of a chosen option (Boorman, Rushworth, & Behrens, 2013; Grabenhorst & Rolls, 2011; Kennerley et al., 2011). Furthermore, this region has been hypothesized to be the merging locus of value coding, where rewarding attributes of stimuli would be encoded in a common currency (Levy & Glimcher, 2012). Accordingly, vmPFC activity seems sufficient to decode the combined value of multi-attribute objects (Kahnt, Grueschow, Speck, & Haynes, 2011) and has been reported for both monetary and primary rewards (Kim, Shimojo, & O'Doherty, 2011). The current finding is consistent with this notion, but for the first time clarifies its strong dissociation with ACC in humans. It shows that its computation is independent of whether the positive outcome was predicted or not, and of whether the option had been intentionally selected or randomly assigned. Besides providing systematic insights on differential ACC and vmPFC functions, these results bridge human functional to primate neurophysiological results (Kennerley et al., 2011).

Furthermore, a main effect of choice was observed in the vmPFC during the outcome phase. The vmPFC was more active for outcomes following actions instructed by the computer (no choice > choice), without interacting with the value coding. This focus on the stimulus (i.e. no choice) features in absence of intentional action (i.e. choice) is in line with what has been proposed as a specialized encoding for stimulus-based value coding, implemented in the vmPFC, as opposed to action-based value coding, processed by the ACC (Camille, Tsuchida, & Fellows, 2011; Rudebeck et al., 2008; Rushworth, Behrens, Rudebeck, & Walton, 2007). The increased action in the vmPFC in this condition across all outcome types might thus derive from the absence of action selection. The potential functional role of this activation might be attentional in nature, with the purpose of underlying that the currently obtained outcome was not a consequence of an intentional choice, and therefore should not influence subsequent strategies (i.e. subsequent intentional choice). Albeit interesting, this interpretation is speculative and should be further addressed in future research. A possible alternative explanation would consider this activity to be Default Mode Network (DMN, Raichle et al., 2001) related. This region is indeed known to be part of the DMN. Moreover one can assume that the No Choice condition is less engaging, and this would justify DMN involvement. However, DMN activity would not coherently explain the outcome-value effect (increased activation for positive outcome). We therefore consider this second option less likely.

Increased activity in the no-choice condition was also observed in the left TPJ. A TPJ contribution is typically detectable whenever an action is performed by an external agent, such as a computer, as compared to when it is internally generated (Spengler, von Cramon, & Brass, 2009; Sperduti, Delaveau, Fossati, & Nadel, 2011). This may correspond to the same distinction between stimulus-based versus action-based value coding; however this interpretation remains speculative and requires further investigation.

Concerning the decision phase, the involvement of the ACC is evidently increased in the choice condition, as compared to the random (i.e. no choice) assignment. This is in line with studies on intentional action, where the ACC is reported as being more active while deciding between two options as opposed to an externally-driven selection (Brass & Haggard, 2007; Demanet, De Baene, Arrington, & Brass, 2013; Forstmann, Brass, Koch, & von Cramon, 2006; Mueller, Brass, Waszak, & Prinz, 2007). The striatum was also more active in the choice condition. This has been previously related to the affective value associated with the possibility of choosing. Leotti and Delgado (2011) reported increased activation in the ventral striatum, while participants were exposed to cues predicting a trial where they could choose. This could potentially explain striatal involvement in our study as well.

The ACC also showed a stronger activation during the decision phase when a risky gamble was selected (low winning probability, high pay-off) as compared to a safe gamble (high winning probability, low pay-off). In other words, a stronger ACC involvement was triggered when people decided to choose a risky gamble over a sure small win, as compared to choosing a safe gamble over the sure small win. This suggests a role for ACC in undertaking a risky behavior. Notwithstanding the speculative nature of this hypothesis, understanding the neural mechanism underlying intentional selection of risky situations (low probability of reward) might provide useful insight with respect to pathological conditions, such as pathological gambling.

Interestingly, the no-choice condition in the decision phase also elicited a bilateral activation in the TPJ, again consistent with agency studies (Farrer & Frith, 2002; Spengler et al., 2009). However, the TPJ activation was mostly unilateral (right) in these studies. This difference may be explained by the increased relevance of our stimuli due to the reward manipulation.

5. Conclusions

The current study systematically investigated mPFC function in encoding three crucial components characterizing goal-directed behavior, namely reward prediction, outcome evaluation, and choice. A striking functional dissociation was detected within the mPFC: While ACC activity reflected reward prediction by signaling positive prediction errors, irrespective of whether the outcome derived from an intentional choice or a randomly selected option, the vmPFC selectively responded to positive outcomes, irrespective of the probability they were linked to. Although this dissociation did not interact with choice condition, vmPFC also carried a neural signature distinguishing between randomly selected (no choice) and intentionally chosen (choice) options. These findings provide new evidence for how complementary but dissociable information that is necessary to drive optimal goal-directed behavior is processed by different subregions within the mPFC.

Acknowledgements

EV, MS, WF and TV were supported by Ghent University GOA grant BOF08/GOA/011. RMK was supported by a post-doctoral fellowship FW011/PDO/016 from the Fund for Scientific Research—Flanders. The authors acknowledge the support of Ghent University Multidisciplinary Research Platform “The integrative neuroscience of behavioral control”.

References

Alexander, W., & Brown, J. W. (2011). Medial prefrontal cortex as an action-outcome predictor. *Nature Neuroscience*, *14*, 1338–1344.

Amiez, C., Joseph, J. P., & Procyk, E. (2006). Reward encoding in the monkey anterior cingulate cortex. *Cerebral Cortex*, *16*(7), 1040–1055, http://dx.doi.org/10.1093/cercor/bhj046.

Bartra, O., Mcguire, J. T., & Kable, J. W. (2013). The valuation system : A coordinate-based meta-analysis of BOLD fMRI experiments examining neural correlates of subjective value. *NeuroImage*, *76*, 412–427.

Blais, C., & Bunge, S. (2010). Behavioral and neural evidence for item-specific performance monitoring. *Journal of Cognitive Neuroscience*, *22*(12), 2758–2767.

Boorman, E. D., Rushworth, M. F. S., & Behrens, T. E. (2013). Ventromedial prefrontal and anterior cingulate cortex adopt choice and default reference frames during sequential multi-alternative choice. *Journal of Neuroscience*, *33*(6), 2242–2253, http://dx.doi.org/10.1523/JNEUROSCI.3022-12.2013.

Botvinick, M. M., Cohen, J. D., & Carter, C. S. (2004). Conflict monitoring and anterior cingulate cortex: An update. *Trends in Cognitive Sciences*, *8*(12), 539–546, http://dx.doi.org/10.1016/j.tics.2004.10.003.

Brass, M., & Haggard, P. (2007). To do or not to do: The neural signature of self-control. *Journal of Neuroscience*, *27*(34), 9141–9145, http://dx.doi.org/10.1523/JNEUROSCI.0924-07.2007.

Brett, M., Anton, J.-L., Valabregue, R., & Poline, J.-B. (2002). Region of interest analysis using an SPM toolbox [abstract]. In: *Presented at the eighth international conference on functional mapping of the human brain* (p. Available on CD-ROM in NeuroImage 16:2).

Bush, G., Vogt, B. A., Holmes, J., Dale, A. M., Greve, D., Jenike, M. A., & Rosen, B. R. (2002). Dorsal anterior cingulate cortex: A role in reward-based decision making. *Proceedings of the National Academy of Sciences of the United States of America*, *99*(1), 523–528, http://dx.doi.org/10.1073/pnas.012470999.

Camille, N., Tsuchida, A., & Fellows, L. K. (2011). Double dissociation of stimulus-value and action-value learning in humans with orbitofrontal or anterior cingulate cortex damage. *Journal of Neuroscience*, *31*(42), 15048–15052, http://dx.doi.org/10.1523/JNEUROSCI.3164-11.2011.

Chib, V. S., Rangel, A., Shimojo, S., & O'Doherty, J. P. (2009). Evidence for a common representation of decision values for dissimilar goods in human ventromedial prefrontal cortex. *Journal of Neuroscience*, *29*(39), 12315–12320, http://dx.doi.org/10.1523/JNEUROSCI.2575-09.2009.

Demanet, J., De Baene, W., Arrington, C. M., & Brass, M. (2013). Biasing free choices: The role of the rostral cingulate zone in intentional control. *NeuroImage*, *72*, 207–213, http://dx.doi.org/10.1016/j.neuroimage.2013.01.052.

Egner, T., Etkin, A., Gale, S., & Hirsch, J. (2008). Dissociable neural systems resolve conflict from emotional versus nonemotional distracters. *Cerebral Cortex*, *18*(6), 1475–1484, http://dx.doi.org/10.1093/cercor/bhm179.

Etkin, A., Egner, T., & Kalisch, R. (2011). Emotional processing in anterior cingulate and medial prefrontal cortex. *Trends in Cognitive Sciences*, *15*(2), 85–93, http://dx.doi.org/10.1016/j.tics.2010.11.004.

Farrer, C., & Frith, C. D. (2002). Experiencing oneself vs another person as being the cause of an action: The neural correlates of the experience of agency. *NeuroImage*, *15*(3), 596–603, http://dx.doi.org/10.1006/nimg.2001.1009.

Forstmann, B. U., Brass, M., Koch, I., & von Cramon, D. Y. (2006). Voluntary selection of task sets revealed by functional magnetic resonance imaging. *Journal of Cognitive Neuroscience*, *18*(3), 388–398, http://dx.doi.org/10.1162/089892906775990589.

Garrison, J., Erdeniz, B., & Done, J. (2013). Prediction error in reinforcement learning: A meta-analysis of neuroimaging studies. *Neuroscience and Biobehavioural Reviews*, *37*, 1297–1310.

Grabenhorst, F., & Rolls, E. T. (2011). Value, pleasure and choice in the ventral prefrontal cortex. *Trends in Cognitive Sciences*, *15*(2), 56–67, http://dx.doi.org/10.1016/j.tics.2010.12.004.

Haber, S. N., & Knutson, B. (2010). The reward circuit: Linking primate anatomy and human imaging. *Neuropsychopharmacology*, *35*(1), 4–26, http://dx.doi.org/10.1038/npp.2009.129.

Hare, T. A., Camerer, C. F., & Rangel, A. (2009). Self-control in decision-making involves modulation of the vmPFC valuation system. *Science*, *324*(5927), 646–648, http://dx.doi.org/10.1126/science.1168450.

Hare, T. A., Doherty, J. O., Camerer, C. F., Schultz, W., & Rangel, A. (2008). Dissociating the role of the orbitofrontal cortex and the striatum in the computation of goal values and prediction errors. *Journal of Neuroscience*, *28*(22), 5623–5630, http://dx.doi.org/10.1523/JNEUROSCI.1309-08.2008.

Holroyd, C. B., & Coles, M. G. H. (2008). Dorsal anterior cingulate cortex integrates reinforcement history to guide voluntary behavior. *Cortex*, *44*(5), 548–559, http://dx.doi.org/10.1016/j.cortex.2007.08.013.

Holroyd, C. B., & Yeung, N. (2012). Motivation of extended behaviors by anterior cingulate cortex. *Trends in Cognitive Sciences*, *16*(2), 122–128, http://dx.doi.org/10.1016/j.tics.2011.12.008.

Jessup, R. K., Busemeyer, J. R., & Brown, J. W. (2010). Error effects in anterior cingulate cortex reverse when error likelihood is high. *Journal of Neuroscience*, *30*(9), 3467–3472, http://dx.doi.org/10.1523/JNEUROSCI.4130-09.2010.

Kahnt, T., Grueschow, M., Speck, O., & Haynes, J.-D. (2011). Perceptual learning and decision-making in human medial frontal cortex. *Neuron*, *70*(3), 549–559, http://dx.doi.org/10.1016/j.neuron.2011.02.054.

Kennerley, S. W., Behrens, T. E. J., & Wallis, J. D. (2011). Double dissociation of value computations in orbitofrontal and anterior cingulate neurons. *Nature Neuroscience*, *14*(12), 1581–1589, http://dx.doi.org/10.1038/nn.2961.

Kennerley, S. W., & Wallis, J. D. (2009). Encoding of reward and space during a working memory task in the orbitofrontal cortex and anterior cingulate sulcus. *Journal of Neurophysiology*, *102*(6), 3352–3364, http://dx.doi.org/10.1152/jn.00273.2009.

Kennerley, S. W., & Walton, M. E. (2011). Decision making and reward in frontal cortex: Complementary evidence from neurophysiological and neuropsychological studies. *Behavioral Neuroscience*, *125*(3), 297–317, http://dx.doi.org/10.1037/a0023575.

Kim, H., Shimojo, S., & O'Doherty, J. P. (2011). Overlapping responses for the expectation of juice and money rewards in human ventromedial prefrontal cortex. *Cerebral Cortex*, *21*(4), 769–776, http://dx.doi.org/10.1093/cercor/bhq145.

Knutson, B., & Cooper, J. C. (2005). Functional magnetic resonance imaging of reward prediction. *Current Opinion in Neurology*, *18*(4), 411–417.

Kool, W., Getz, S. J., & Botvinick, M. M. (2013). Neural representation of reward probability : Evidence from the illusion of control. *Journal of Cognitive Neuroscience*, *25*(6), 852–861, http://dx.doi.org/10.1162/jocn.

Leotti, L. A., & Delgado, M. R. (2013). The inherent reward of choice. *Psychological Science*, *22*(10), 1310–1318, http://dx.doi.org/10.1177/0956797611417005.

Levy, D. J., & Glimcher, P. W. (2012). The root of all value: A neural common currency for choice. *Current Opinion in Neurobiology*, *22*(6), 1027–1038, http://dx.doi.org/10.1016/j.conb.2012.06.001.

Liu, X., Hairston, J., Schrier, M., & Fan, J. (2011). Common and distinct networks underlying reward valence and processing stages: A meta-analysis of functional neuroimaging studies. *Neuroscience and Biobehavioral Reviews*, *35*(5), 1219–1236, http://dx.doi.org/10.1016/j.neubiorev.2010.12.012.

Matsumoto, M., Matsumoto, K., Abe, H., & Tanaka, K. (2007). Medial prefrontal cell activity signaling prediction errors of action values. *Nature Neuroscience*, *10*(5), 647–656, http://dx.doi.org/10.1038/nn1890.

Mueller, V. A., Brass, M., Waszak, F., & Prinz, W. (2007). The role of the preSMA and the rostral cingulate zone in internally selected actions. *NeuroImage*, *37*(4), 1354–1361, http://dx.doi.org/10.1016/j.neuroimage.2007.06.018.

Nee, D. E., Kastner, S., & Brown, J. W. (2011). Functional heterogeneity of conflict, error, task-switching, and unexpectedness effects within medial prefrontal cortex. *NeuroImage*, *54*(1), 528–540, http://dx.doi.org/10.1016/j.neuroimage.2010.08.027.

Noonan, M. P., Kolling, N., Walton, M. E., & Rushworth, M. F. S. (2012). Re-evaluating the role of the orbitofrontal cortex in reward and reinforcement. *European Journal of Neuroscience*, *35*(7), 997–1010, http://dx.doi.org/10.1111/j.1460-9568.2012.08023.x.

O'Doherty, J. P., Deichmann, R., Critchley, H. D., & Dolan, R. J. (2002). Neural responses during anticipation of a primary taste reward. *Neuron*, *33*(5), 815–826.

Padoa-Schioppa, C., & Assad, J. A. (2008). The representation of economic value in the orbitofrontal cortex is invariant for changes of menu. *Nature Neuroscience*, *11*(1), 95–102, http://dx.doi.org/10.1038/nn2020.

Plassmann, H., O'Doherty, J., & Rangel, A. (2007). Orbitofrontal cortex encodes willingness to pay in everyday economic transactions. *Journal of Neuroscience*, *27*(37), 9984–9988, http://dx.doi.org/10.1523/JNEUROSCI.2131-07.2007.

Platt, M. L., & Huettel, S. A. (2008). Risky business: The neuroeconomics of decision making under uncertainty. *Nature Neuroscience*, *11*(4), 398–403, http://dx.doi.org/10.1038/nn2062.

Raichle, M. E., MacLeod, A. M., Snyder, A. Z., Powers, W. J., Gusnard, D. A., & Shulman, G. L. (2001). A default mode of brain function. *Proceedings of the National Academy of Sciences of the United States of America*, *98*(2), 676–682, http://dx.doi.org/10.1073/pnas.98.2.676.

Rainville, P. (1997). Pain affect encoded in human anterior cingulate but not somatosensory cortex. *Science*, *277*(5328), 968–971, http://dx.doi.org/10.1126/science.277.5328.968.

Rangel, A., & Hare, T. (2010). Neural computations associated with goal-directed choice. *Current Opinion in Neurobiology*, *20*(2), 262–270, http://dx.doi.org/10.1016/j.conb.2010.03.001.

Rudebeck, P. H., Behrens, T. E., Kennerley, S. W., Baxter, M. G., Buckley, M. J., Walton, M. E., & Rushworth, M. F. S. (2008). Frontal cortex subregions play distinct roles in choices between actions and stimuli. *Journal of Neuroscience*, *28*(51), 13775–13785, http://dx.doi.org/10.1523/JNEUROSCI.3541-08.2008.

Rushworth, M. F. S., & Behrens, T. E. J. (2008). Choice, uncertainty and value in prefrontal and cingulate cortex. *Nature Neuroscience*, *11*(4), 389–397, http://dx.doi.org/10.1038/nn2066.

Rushworth, M. F. S., Behrens, T. E. J., Rudebeck, P. H., & Walton, M. E. (2007). Contrasting roles for cingulate and orbitofrontal cortex in decisions and social behaviour. *Trends in Cognitive Sciences*, *11*(4), 168–176, http://dx.doi.org/10.1016/j.tics.2007.01.004.

Rushworth, M. F. S., Kolling, N., Sallet, J., & Mars, R. B. (2012). Valuation and decision-making in frontal cortex: One or many serial or parallel systems? *Current Opinion in Neurobiology*, *22*(6), 946–955, http://dx.doi.org/10.1016/j.conb.2012.04.011.

Rushworth, M. F. S., Noonan, M. P., Boorman, E. D., Walton, M. E., & Behrens, T. E. (2011). Frontal cortex and reward-guided learning and decision-making. *Neuron*, *70*(6), 1054–1069, http://dx.doi.org/10.1016/j.neuron.2011.05.014.

Schoenbaum, G., Roesch, M. R., Stalnaker, T. A., & Takahashi, Y. K. (2009). A new perspective on the role of the orbitofrontal cortex in adaptive behaviour. *Nature Reviews. Neuroscience*, *10*(12), 885–892, http://dx.doi.org/10.1038/nrn2753.

Sescousse, G., Caldú, X., Segura, B., & Dreher, J. (2013). Processing of primary and secondary rewards: A quantitative meta-analysis and review of human functional neuroimaging studies. *Neuroscience & Biobehavioral Reviews*, *37*, 681–696.

Shackman, A. J., Salomons, T. V., Slagter, H. A., Fox, A. S., Winter, J. J., & Davidson, R. J. (2011). The integration of negative affect, pain and cognitive control in the cingulate cortex. *Nature Reviews. Neuroscience*, *12*(3), 154–167, http://dx.doi.org/10.1038/nrn2994.

Silvetti, M., Seurinck, R., & Verguts, T. (2011). Value and prediction error in medial frontal cortex: Integrating the single-unit and systems levels of analysis. *Frontiers in Human Neuroscience*, *49*(6), 1627–1635, http://dx.doi.org/10.3389/fnhum.2011.00075.

Silvetti, M., Seurinck, R., & Verguts, T. (2013). Value and prediction error estimation account for volatility effects in ACC: A model-based fMRI study. *Cortex*, *49*(6), 1627–1635, http://dx.doi.org/10.1016/j.cortex.2012.05.008.

Spengler, S., von Cramon, D. Y., & Brass, M. (2009). Was it me or was it you? How the sense of agency originates from ideomotor learning revealed by fMRI. *NeuroImage*, *46*(1), 290–298, http://dx.doi.org/10.1016/j.neuroimage.2009.01.047.

Sperduti, M., Delaveau, P., Fossati, P., & Nadel, J. (2011). Different brain structures related to self- and external-agency attribution: A brief review and meta-analysis. *Brain Structure & Function*, *216*(2), 151–157, http://dx.doi.org/10.1007/s00429-010-0298-1.

Sul, J. H., Kim, H., Huh, N., Lee, D., & Jung, M. W. (2010). Distinct roles of rodent orbitofrontal and medial prefrontal cortex in decision making. *Neuron*, *66*(3), 449–460, http://dx.doi.org/10.1016/j.neuron.2010.03.033.

Sutton, R. S., & Barto, A. G. (1998). *Reinforcement learning : An introduction*. Cambridge, MA: MIT Press (MIT Press, Cambridge, MA).

Tom, S. M., Fox, C. R., Trepel, C., & Poldrack, R. A. (2007). The neural basis of loss aversion in decision-making under risk. *Science*, *315*(5811), 515–518, http://dx.doi.org/10.1126/science.1134239.

Vassena, E., Silvetti, M., Boehler, C. N., Achten, E., Fias, W., & Verguts, T. (2014). Overlapping neural systems represent cognitive effort and reward anticipation. *PLoS One*, *9*(3), e91008, http://dx.doi.org/10.1371/journal.pone.0091008.

Venkatraman, V., & Huettel, S. A. (2012). Strategic control in decision-making under uncertainty. *European Journal of Neuroscience*, *35*(7), 1075–1082, http://dx.doi.org/10.1111/j.1460-9568.2012.08009.x.

Wager, T. D., Lindquist, M., & Kaplan, L. (2007). Meta-analysis of functional neuroimaging data: Current and future directions. *Social Cognitive and Affective Neuroscience*, *2*(2), 150–158, http://dx.doi.org/10.1093/scan/nsm015.

Woo, C.-W., Krishnan, A., & Wager, T. D. (2014). Cluster-extent based thresholding in fMRI analyses: Pitfalls and recommendations. *NeuroImage*, *91*, 412–419, http://dx.doi.org/10.1016/j.neuroimage.2013.12.058.